From the Rothamsted Experimental Station, Harpenden, Herts. (England) and University of Granada (Spain)

Fourier Transform Methods for Studying Scattering from Lamellar Systems

I. A Direct Method for Analysing Interstratified Mixtures

By Douglas M. C. MacEwan

With 8 figures in 14 details and 5 tables (Received January 16, 1956)

1. Introduction

Of recent years the problem of interstratification in clay minerals has assumed considerable importance. Many of these minerals are composed of well-marked layer structures, and the layers belong to a limited range of types, all of which can be regarded as built up from only two fundamental structural units — the octahedral layer, resembling that of brucite and gibbsite, and the tetrahedral layer, which does not occur separately in any natural mineral, but is related to the cristobalite structure. It is impossible here to describe these structural types in detail; suitable specialised works may be consulted (1, 2, 3).

The layers may occur in nature with various degrees of interlamellar hydration — i. e. with water layers between them — and also with various degrees of what I have called (3a) "chloritization" — i. e., brucitic, or perhaps gibbsitic type hydroxide layers between the silicate layers. Some artificially activated (acid-treated) clay minerals also probably have silica in interlamellar positions (4).

It has become increasingly clear that natural minerals may contain various structural units of this type mixed up in a random (but sometimes also in a regular) manner — as if a pack of cards were formed of two or three types shuffled together. It is important to have suitable methods for interpreting the diffraction effects given by such interstratified mixtures. Since the people who are interested in them are often geologists, soil scientists, and others with no specialised knowledge of X-ray crystallography, these methods should be easy to apply. There is a fundamental difficulty resulting from the fact that the interpretation of the X-ray diagrams is a structural problem, whereas, from the investigator's point of view it is a matter of identification — and there is a great difference in the time factor allowable for these two approaches.

Important fundamental calculations for such structures were published by Hendricks and Teller in 1942 (5). They were probably used very little at that time, being beyond the grasp of noncrystallographers. The present author, with G. Brown (6) has calculated from Hendricks and Teller's formulae a series of curves illustrating the diffraction to be expected from various mixtures likely to occur in practice. These calculations have been to some extent checked experimentally (7) and the curves have undoubtedly been found useful in many investigations.

However, it is impossible with such a set of curves to provide for all the variations likely to occur in actual minerals. In fact they were only calculated for two-component systems of large crystallite size, although in practice applicable to a rather wider range of types.

For this reason, a direct method based on Fourier transforms has been applied to several problems of this nature by the present author (8, 9). Experience has shown it to have considerable scope, such as to warrant giving a fuller description than it has received. This is the aim of the present paper.

2. Nature of the problem

We are concerned here solely with the problem of identification defined above. In its general form, this consists of finding the manner of distribution of interlayer spacings in the material under consideration (which may be, and frequently is, a mixture of minerals, often however genetically related).

The meaning of the term "mixture" is not immediately clear in this connexion, and it has to be defined. It means a "mechanical" mixture, i. e. one in which crystallites of different nature are present. Each of the crystallite types may be itself an interstratification of two or more types of layer, i. e. a "mixed-layer" crystallite; so that a given mineral may be a "mechanical" mixture of "mixed-layer" crystallites. This is a very complex case. More often, one sort of mixed-layer crystallite is present, the other components being readily-recognizable pure minerals.

To make these ideas more precise, let us take an example. A quite commonly occurring case is to have a mixture of a mica (spacing between layers about 10 Å), a vermiculite (spacing between layers variable, but about 14 Å in fully hydrated state), and an interstratification of the two. Since the basic layer structure of vermiculite is micaceous, there may well be a genetic relationship between the components. Also, the interstratified crystals may be regarded as being composed of similar layers separated by interlayer distances, sometimes of 10, sometimes of 14 Å. No other interlayer distances will occur.

In general it may always be assumed that only a limited (and quite small) number of different interlayer distances can occur in such minerals, and that the layers in any crystallite are strictly parallel, and usually similar in nature. The problem is to find the law of distribution of the interlayer distances.

Other examples of possible mixed-layer crystal are:
Partially hydrated halloysite (10)
(spacings 7·2 and 10 Å).
Mica and montmorillonoid[1])
(spacings 10 and 12–18 Å).
Partially hydrated labile chlorite (12)
(spacings 14 and 18 Å).
Various organic complexes with montmorillonite (13, 14)
(various spacings between 10 and 22 Å or even more).

Apart from clay minerals — the most important application at present — problems of an essentially similar type occur in interpreting the diffraction diagrams from other lamellar systems, for instance graphitic acid (15, 16), α-zinc hydroxide (17), etc.

The markedly lamellar nature of all these minerals makes it easy to obtain parallel orientation to the cleavage flakes (it must be remembered that they are much too small to handle individually). There are various ways of doing this, such as allowing a suspension to settle on glass (18), applying pressure (19), centrifuging (20), etc. By suitable mounting of the specimen (21) it is then usually easy to obtain the basal, or (001)[2]) series of reflections almost clear of disturbing reflections of other types. At any rate, this can usually be done well enough to determine the positions and intensities of the main peaks, and to get an idea of their shape, though techniques are seldom delicate enough (even if time were available) for a full analysis of the total distribution of scattering from the basal planes. Our problem then is to obtain the maximum amount of information from the data readily available. It is essentially one of identification, rather than of structure analysis, so some method which is rapid, and not too difficult to apply, is needed.

It should be realised that the layers are usually quite large in extent (say some hundreds to some thousands of Å in diameter), so that they are represented by narrow rods in reciprocal space. Problems of integration throughout the volume of a broad reciprocal rod, such as occur in dealing with amorphous carbons, for instance, are not considered here [some similar problems have however been treated by Méring and Brindley (22)].

Generally speaking, the existence of random interstratification in such material is betrayed by the presence of a non-rational series of basal reflection. Such reflections, as has been pointed out by Méring (23) are not necessarily more diffuse than those given by regularly crystallised material, since reflections from clay minerals are generally broadened in any case due to small particle size of the material, and various irregularities in crystallisation, or a different type from those discussed here.

The problem with which we are faced is to find the inter-layer spacings which exist in the mixture, the proportions in which they are present, and the manner of their distribution (i. e. whether completely randomly distributed; or completely segregated; or something between the two). It is convenient for this purpose to consider one layer and its associated interlamellar molecules (on one arbitrarily chosen side) as constituting a complex layer, and the whole mixture as being made up of a number of such layers, n different varieties being present. We define the probability of occurrence of a layer of type r as p_r; and the probability that type s succeeds type r (again moving in an arbitrary but defined direction) as p_{rs}.
Clearly then

$$\Sigma_r p_r = 1 \qquad [1a]$$

$$\Sigma_s p_{rs} = 1, \quad \text{for all } r. \qquad [1b]$$

We shall show later that we also have the relation

$$\Sigma_r p_r p_{rs} = p_s, \quad \text{for all } s. \qquad [1c]$$

A knowledge of the values of the p_r and p_{rs} then completely defines the system.

As an example, we may take the two-component system with equal amounts of the two components, so

[1]) This term was introduced provisionally by the present author (11) to mean any mineral of the montmorillonite group. The term "montmorin" (introduced by Correns) has also been used widely in this sense; and recently, at the International Crystallographic Congress in Paris, 1954, the British Clay Minerals Group has proposed the term "smectite".

[2]) In the case of mixed-layer minerals, unique l-indices cannot be assigned, but it may still be useful to make use of such indices (see ref. 6).

that $p_1 = p_2 = 1/2$. Then, for the completely random case

$$p_{11} = p_{12} = p_{22} = 1/2.$$

For the case of complete segregation (separate regular crystallites)

$$p_{11} = p_{22} = 1, \quad p_{12} = 0.$$

There is also the possibility of a regular succession of layers of the two types 1212···, forming a single type of regular crystal. For this case

$$p_{11} = p_{22} = 0, \quad p_{12} = 1.$$

All intermediate cases are of course possible.

It will be noticed that this type of definition of the p's does not allow for any influence of a layer on other than neighbouring layers. Thus the sort of structure represented by 112112112··· cannot be represented at all, with any value of the p's.

3. Derivation of Fourier transform

The Fourier transform method is closely analogous to the well-known technique for determining the radial distribution in a liquid. Certain modifications are however necessary, since we are here dealing with a linear, and not a radial, distribution. We start with the formula, which is developed on p. 464 of James (24).

$$|A|^2 = C\left\{A_0 + \Sigma_p \Sigma_q f_p f_q^* \quad e^{iK\boldsymbol{S}\cdot\boldsymbol{r}_{pq}}\right\} \qquad [2]$$

Here p, q are atoms and f_p, f_q the corresponding atomic scattering factors; $\boldsymbol{r}_{pq}$ is an interatomic vector, $\boldsymbol{S}$ the unit vector defining the scattering conditions; K is $2\pi/\lambda$.

Now let us consider a layer structure, having layers with the layer form factor F_π say, so that

$$F_\pi = \Sigma'_p f_p e^{iK\boldsymbol{r}_p\cdot\boldsymbol{S}} \qquad [3]$$

where Σ' indicates a sum over all the atoms belonging to the layer. The sum above can thus be split into within-layer sums (which depend only on the nature of the layer) and between-layer sums. In the latter we can substitute

$$\boldsymbol{r}_{pq} = \boldsymbol{r}'_{pq} + \boldsymbol{R}_{\pi\varrho} + \boldsymbol{\zeta}_{\pi\varrho} \qquad [4]$$

where $\boldsymbol{r}'_{pq}$ is the within-layer distance corresponding to $\boldsymbol{r}_{pq}$; $\boldsymbol{R}$ is the perpendicular distance between the layers π and ϱ; and $\boldsymbol{\zeta}_{\pi\varrho}$ is the lateral shift of one layer over the other. We thus get

$$|A|^2 = C\left\{A_0 + \Sigma_\pi \Sigma_\varrho F_\pi F_\varrho^* \; e^{iK\boldsymbol{S}\cdot(\boldsymbol{R}_{\pi\varrho}+\boldsymbol{\zeta}_{\pi\varrho})}\right\} \qquad [5]$$

where each of the sums includes the case $\pi = \varrho$.

The layers are assumed identical, so this becomes simply

$$\frac{|A|^2}{C} = A_0 + \Sigma_{\pi\varrho} |F|^2 \; e^{iK\boldsymbol{S}\cdot(\boldsymbol{R}_{\pi\varrho}+\boldsymbol{\zeta}_{\pi\varrho})} \qquad [6]$$

($|F|^2$ is of course a function of angle).

We can simplify the expression by taking

$$\boldsymbol{R}_{\pi\varrho} = \boldsymbol{L}\cdot R_{\pi\varrho} \qquad [7]$$

where $\boldsymbol{L}$ is a unitary vector defining the orientation of the layer aggregate and $R_{\pi\varrho}$ is a scalar distance.

We now introduce the probability function $\omega(R)$ such that the probability of one layer in any range dl_π and one layer in dl_ϱ with separation $R_{\pi\varrho}$ is $(R_{\pi\varrho})\,dl_\pi dl_\varrho / T^2$, T being the total thickness of the aggregate.

Thus

$$\frac{|A|^2}{C} = A_0 + N^2|F|^2 \int\int \omega(R_{\pi\varrho})\, e^{iK\boldsymbol{S}\cdot(\boldsymbol{L}\cdot R_{\pi\varrho}+\zeta_{\pi\varrho})} \frac{dl_\pi\, dl_\varrho}{T^2}. \qquad [8]$$

The first (zero-order) term dies out rapidly with angle, and may be neglected. The second term, if integrated once, gives unity, as in the case of liquid diffraction (Ref. 24, p. 469), on the assumption that there is an equal probability of finding any layer at any point in a particle. We are thus left with

$$\frac{|A|^2}{C} = \frac{N^2|F|^2}{T} \int \omega(R)\; e^{i\mu(R\cos\alpha + \sigma_{\pi\varrho}\cos\beta)}\, dR. \qquad [9]$$

Here $\mu = 4\pi(\sin\Theta)/\lambda$: α is the angle between the Ewald vector and the normal to the layers: $\sigma_{\pi\varrho}$ is the (scalar) shift of the ϱ layer with respect to the π layer, in the plane of the layer: β is the angle between the direction of this shift and the Ewald vector.

The imaginary part of the above integral must cancel out, since the intensity I is real. Also we may suppose that $\omega \to 1$ as $R \to \infty$ i. e. that the crystallites have a finite size, so that beyond a certain value of R there are no interlayer distances. Thus

$$\frac{|A|^2}{C} = \frac{2N|F|^2}{T} \int_0^\infty \omega(R)\cos(\mu R\cos\alpha + \mu\sigma\cos\beta)\, dR. \qquad [10]$$

Since we are considerung the case of "specular" reflection from an oriented aggregate, $\cos\alpha = 1$ and $\cos\beta = 0$, so that

$$\frac{\bar{I}_l}{|F|^2} = \frac{2}{a} \int_0^\infty \omega(R)\cos\mu R\, dR. \qquad [11]$$

Here a is the mean thickness of a layer $= T/N$. The difference between N and $N-1$ is neglected. $\bar{I}_l$ is the mean intensity of scattering by a single layer (for the particular value of μ considered), divided by the geometrical factor C.

If the expression on the left-hand side of [11] is represented for brevity by $i(\mu)$, then on transforming the integral we get

$$\omega(R) = \frac{a}{\pi} \int_0^\infty i(\mu)\cos\mu R\, d\mu \qquad [12]$$

which gives the probability function directly from the observations.

It will be noted, that in contrast to the formula for radial distribution in a liquid (Ref. 24, p. 497), this is a cosine transform, and not a sine transform. This is because the one-dimensional distribution does not involve any spatial integration. Also, this function involves the measured intensities directly, and not their "complements" $(\bar{I}_a/|F|^2 - 1)$. Finally, if plotted as a function of R, this formula gives a maximum at the origin, and not a zero value. This is because formula [8] includes the case $\pi = \varrho$; the maximum merely expressed the fact that every layer is at zero distance from itself. Our function is thus rather analogous to a Patterson series in one dimension.

the contribution of this peak to the Fourier integral is

$$\frac{a}{\pi} \frac{I_s}{|F_s|^2} \cos \mu_s R \qquad [14]$$

where F_s is the value of F at the peak. This is assumed to be approximately constant over the whole area of the peak. Thus the formula for the transform becomes

$$\omega(R) = \Sigma_s \frac{a}{\pi} \frac{I_s}{|F_s|^2} \cos \mu_s R. \qquad [15]$$

The analogy to a Patterson series is very clear from this form of the transform. It is in fact a Patterson series with non-rational coordinates (the μ_s), i. e. with no definite unit cell. We may if we like regard it as being the Patterson series corresponding to a very large unit cell (larger than any interlayer-vectors we expect to find). This series,

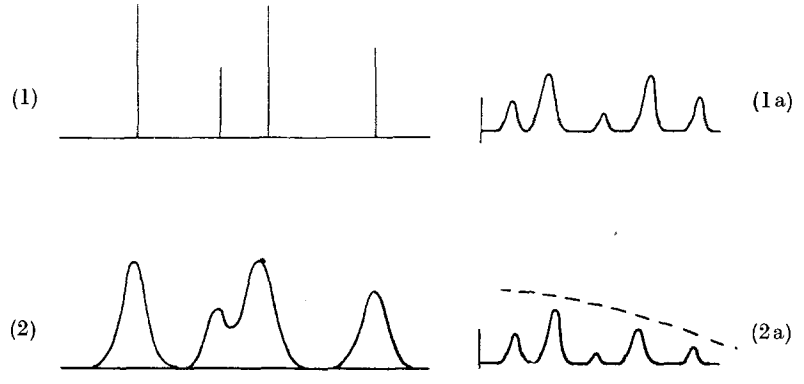

Fig. 1. (1) Ideal case of sharp isolated reflexions, giving the transform $\omega(R) = \Sigma_s i_s \cos 2\pi \mu_s R$. This curve is shown in [1a] — (2) Broadened reflexions of error curve type, and of uniform width (standard deviation), giving the transform $\omega(R) = e^{-\frac{1}{2}\sigma^2 R^2} \Sigma_s i_s \cos 2\pi \mu_s R$. This curve is shown in [2a].

If, as often happens, we have a diagram consisting of a series of fairly sharp lines, but not forming a "rational" sequence, the entire variation of the function $\bar{I}_l/|F_l|^2$ may not be really observable; we thus cannot calculate the complete Fourier transform, even if the labor involved were acceptable. We can however measure accurately the positions of the diffraction maxima, and with fair accuracy their relative intensities. We can now express the equation [12] in such a way that it makes use of this information directly. Let us define the "intensity" of a line by the expression

$$I_s = \int_{\mu_s - \delta\mu}^{\mu_s + \delta\mu} I \, d\mu \qquad [13]$$

the integration being performed over a small region which includes the whole peak. Then in general, never repeats: however, errors accumulate as we go to large values of R, and it becomes progressively less reliable.

4. The case of broad peaks

The approximation used here, of replacing each peak (which may be quite a diffuse one) with a single term, may seem to be excessively drastic.

Let us suppose therefore that each peak, instead of being represented by a single line [fig. 1(1)], is represented by a distribution of intensity having the form of a Gaussian curve [fig. 1 (2)]. If μ_s is the coordinate (reciprocal spacing) at the center of such a peak, the distribution is

$$\frac{1}{\sigma\sqrt{2\pi}} e^{-\frac{1}{2\sigma^2}(\mu - \mu_s)^2} = f_s(\mu) \qquad [16]$$

and the Fourier transform of this peak is given by

$$\int_{-\infty}^{+\infty} f_s(\mu) \cos \mu R \, d\mu = e^{-\frac{1}{2}\sigma^2 R^2} \cos \mu_s R. \quad [17]$$

In our case therefore, if the peaks all have the same widths (same σ), we get

$$\omega(R) = e^{-\frac{1}{2}\sigma^2 R^2} \Sigma_s A_s \cos \mu_s R \quad [18]$$

where A_s is proportional to the height of the sth peak.

Essentially, this gives a transform of the same general shape as that given by a series of "line peaks" but dying out with distance from the origin, as given by the factor $e^{-\frac{1}{2}\sigma^2 R^2}$ [fig. 1 (2a)].

If each μ_s has a different σ_s (i. e. if the peaks have different widths), we get

$$\omega(R) = \Sigma_s A_s \, e^{-\frac{1}{2}\sigma_s^2 R^2} \cos \mu_s R \quad [19]$$

and the attenuation factor is different for each term of the summation. It is not difficult to make this calculation (the Fourier components, instead of being added "as received", are first attenuated by various factors depending on R), but the extra complication is probably seldom worth while.

For a rather broad peak, for example, the "half width" might be 2/100 in reciprocal units, and $\sigma \cdot = .1/100$, so that the coefficient of attenuation would be 0.95 at $R = 30$ Å. This means that, even for quite broad peaks, the effect of peak width is likely to be unimportant.

This treatment does not take account of "skewness" of the peaks, or of the variation of structure factor within the region of a peak (which is, in fact, one of the factors giving rise to skewness). In certain cases, these factors may be important. It explains however why quite surprisingly good results may be obtained, even with rather diffuse peaks.

5. Interpretation of the transform

The Fourier transform consists of a curve with peaks at distinct values of R, these peaks corresponding to prominent inter-layer distances. In theory these peaks are extremely sharp, for in the type of complexes we are considering, the inter-layer distances are definite. In practice however the peaks are found to have a certain width, so that if two inter-layer distances occur close together (say 28 and 30 Å), there may be some difficulty in separating them. The reason for this is that only a certain number of the diffraction maxima are available to us, i. e. those corresponding to $\mu < \mu_m$, where μ_m is the maximum conveniently observable value of reciprocal spacing.

Fig. 1 may represent this case, if we imagine the transform and the intensity function interchanged. We now suppose the intensity values to have a progressive diminution superposed on them [represented by the dotted line in fig. 1 (2a)]. The result is that the Fourier transform, which should have absolutely sharp peaks as in fig. 1 (1), in fact has peaks of a certain width as in fig. 1 (2). The intensity is more likely to have a sharp "cut-off" rather than a superposed gradual fall. The result of this will be, as is well known, that a strong peak will be bordered by parasitic "diffraction" peaks, at a distance of about $2/\mu_m$. These parasitic peaks are usually particularly noticeable near the big peak at $R = 0$, where they usually cause no trouble, and are easily recognised. They may be eliminated, or greatly reduced, by superimposing a gradual fall of intensity (which ideally should have the form of a Gaussian curve) on the observed series of intensities. This may be a useful means of checking on the reality of a given peak on the Fourier transform diagram; an example is given below.

Assuming that the "cut-off" point μ_m corresponds to an attenuation of about $1/e$, it can be shown that the "half-width" of the resulting peaks on the Fourier transform is about $2/\mu_m$ Å. If, for instance, we are able to observe diffraction effects down to about 2 Å ($\mu_m = 0.5$), the peaks have a "half-width" of about 4 Å, so that it would be difficult to separate peaks at 28 and 30 Å on the Fourier transform, if "modified" intensity data (with a gradual fall superimposed) were used. Using unmodified data, peaks as close together as this could generally be resolved, at the expense of getting some spurious effects; by calculating both series, and comparing them (not a very arduous task) these spurious effects could be picked out without difficulty.

Since the Fourier transform represents $\omega(R)$, the area of each peak may be taken to represent the relative probability of the occurrence of that spacing. Since further the width of the peaks is constant, heights may be used instead of areas, except insofar as partially superposed peaks may occur. Whether heights or areas are used however, a difficulty occurs in that we do not know the

correct base line for the peaks. This happens because the zero-order term has been omitted from the summation. It corresponds to a constant which has to be added to all the terms in the summation.

Nearly always, the correct zero-level can be drawn in with sufficient accuracy by inspection of the curve, especially the region near $R = 0$. There are usually no genuine peaks in this region, except for the very large peak at the origin. Associated with it, it is usually possible to see two diffraction peaks. The base line is drawn in so as to cut off approximately equal areas from these diffraction peaks, above and below (see fig. 6 for an example of this).

It is also possible to calculate the position of the base line, in the following way. We have

$$\omega(R) = \Sigma_s i_s \cos \mu_s R,$$

where $i_s = (a/\pi)\ (I_s/|F_s|^2)$.

Hence

$$\frac{1}{T}\int_0^T \omega(R)dR = \frac{1}{T}\Sigma_s i_s \int_0^T \cos \mu_s R\, dR. \quad [20]$$

The integral on the right hand side is practically zero except when $\mu_s = 0$, when it equals T. Hence

$$i_0 = \frac{1}{T}\int_0^T \omega(R)dR. \quad [21]$$

But the density of peaks in the $\omega(R)$ curve will be about the same for any region $\Delta R \gg a$ and $< T$. Thus we can say that

$$i_0 \doteq \frac{1}{R_2 - R_1}\int_{R_1}^{R_2} \omega(R)dR. \quad [22]$$

This gives the following rule for finding i_0. Draw an approximate base-line on the curve of $\omega(R)$, and sum the total area of the peaks in any fairly large range ΔR. This can be done approximately by measuring their heights, and their widths at the base, and treating them as equilateral triangles; or, if a planimeter is used, the total area above the base-line can be measured accurately, neglecting obvious false "diffraction" peaks (this is better than reckoning the "algebraic" area, reckoning regions below the provisional baseline as negative).

The relations [1a—c], given in section 2 place severe limitations on the choice of the probability coefficients, p_{rs}. If there are n components in the mixture, the number of such coefficients is n^2, and the number of equations is n of type [1b] and n of type [1c], i. e. $2n$ in all. However, these only provide $2n - 1$ independent conditions, since from each set of equations we may derive an identical equation, making use of [1a]. Thus, multiplying [1b] by p_r and summing we get:

$$\Sigma_r \Sigma_s p_r p_{rs} = \Sigma_r p_r = 1, \text{ by [1a]};$$

and from [1c]:

$$\Sigma_r \Sigma_s p_r p_{rs} = \Sigma_s p_s = 1, \text{ by [1a]}.$$

Thus the number of independent conditions is $2n - 1$, so that the number of degrees of freedom in the p_{rs} is $n^2 - 2n + 1$.

In the case, for instance, of a two-component mixture, we have six coefficients p_A, p_B, p_{AA}, p_{AB}, p_{BA}, p_{BB}. But only two of these are independent. First of all, from [1a], $p_B = 1 - p_A$. Then, the application of [1b] and [1c] leaves us with $4 - 4 + 1 = 1$ degree of freedom for the other four constants.

The most convenient procedure, perhaps, is to seek constants satisfying [1b] (this can be done very readily), and also in general accord with the peak heights. Conditions [1c] can then be used as a check on the reasonableness of the set of coefficients, which if necessary can be suitable adjusted. If they cannot be so adjusted, then the interpretation must be wrong.

Peak areas (or heights) are proportional to the probability of finding the corresponding interlayer spacing in the mixture, or, what is the same thing, to the number of times it occurs. Thus, if h represents peak height, we have, for the "primary" or "fundamental" peaks, i. e. those representing spacings between contiguous layers, $h_r = p_r$ (omitting a proportionality factor), and for the "secondary" or "combination" peaks (which represent spacings between layers separated by other layers).

$$h_{rr} = p_r p_{rr} \quad [23]$$

$$h_{rs} = p_r p_{rs} + p_s p_{sr} \quad [24]$$

(since h_{rs} is of course really $h_{rs} + h_{sr}$).

$$h_{r\,n\,\boldsymbol{hrn}} = p_r p_{rr}^{n-1}. \quad [25]$$

Other coefficients are more difficult to calculate, but the general principles can be seen from the following examples:

$$h_{ABC} = p_A (p_{AB} p_{BC} + p_{AC} p_{CB}) + p_B (p_{BA} p_{AC} + p_{BC} p_{CA}) + p_C (p_{CA} p_{AB} + p_{CB} p_{BA}).$$

$$h_{AAB} = p_A (p_{AA} p_{AB} + p_{AB} p_{BA}) + p_B (p_{BA} p_{AA}).$$

Condition [25] means that, in a random mixture, with no influence of a layer on non-neighboring layers, the peaks A, AA, AAA, ... are in the ratio $1 : p_{AA} : p_{AA}^2 : \ldots$. This is not the case if ordering with non-nearest-neighbor interaction is permitted. Forinstan-

ce, in the structure $AAABAAABAAAB\ldots$, we have $p_A = 0.75$, $p_{AA} = 0.67$, $p_{AAA} = 0.33$, $p_{A^4} = p_{A^5} = \ldots = 0$, so that:

$$h_{AA}/h_A = 0.89$$
$$h_{AAA}/h_{AA} = 0.5$$
$$h_{A^4}/h_{AAA} = 0$$

Sometimes it is useful to remove strong peaks which mask the positions of others. Such peaks may also – for the reasons already stated – be surrounded by "diffraction" effects, which confuse the diagram. Their removal may be effected as follows.

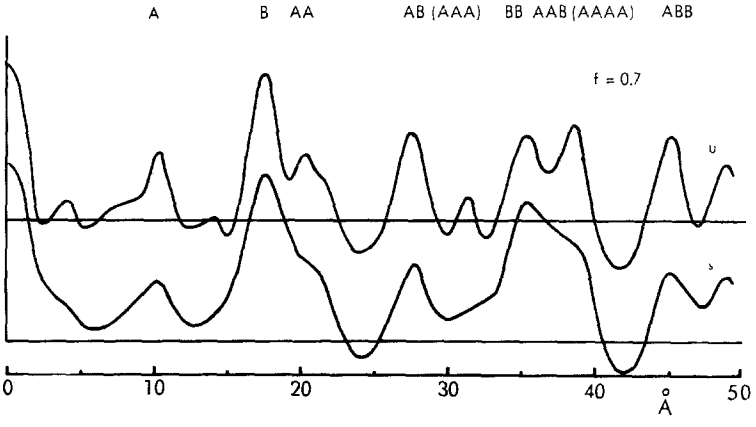

Fig. 2. Transform from calculated intensities for 10 : 17.7 Å mixture (mica-montmorillonoid) in ratio 0.3 : 0.7. Above, unsmoothed; below, smoothed

Let us suppose that the peaks we want to remove are at $R_1, R_2, \ldots$, and that their areas are $A_1, A_2, \ldots$ We calculate the "intensity" corresponding to those peaks alone, by means of the Fourier transform

$$i_p = \frac{2}{a} \Sigma_m A_m \cos \mu R_m \ldots \quad [24]$$

This intensity function will have a series of peak values, the associated total (integrated) intensities being, say, $i_{p1}, i_{p2}, \ldots$ We then introduce these intensities with negative sign into the calculation of the Fourier transform, the other terms being, of course, the experimental i's. In this way, we remove the unwanted peaks, and the associated "diffraction" effects.

6. Some practical examples

As a first example of the practical application of this method, we will take an artificially constructed case, since it is simple, and illustrates well the features of the method.

Brown and the author (6) have published calculated scattering curves [according to the formula of Hendricks and Teller (5)] for various completely random mixtures. From these curves we may derive peak heights and intensities, and calculate Fourier transforms. Fig. 2 shows two transforms (above, unsmoothed and below, smoothed) for a 10 Å: 17.7 Å mixture (corresponding to mica, and glycerol-montmorillonoid) in proportion 3 : 7. Table 1 gives the spacings and intensities used. The zero line has been determined by the method given in the preceding section. It is clear that it could, in fact, have been drawn in at sight with very fair accuracy.

Looking at the transforms, we see at once that certain peaks (those at c. 4, 14, 32 Å) are spurious and may be rejected. The peak at around 4 Å is a constant feature of this type of diagram, being due to diffraction by the very large peak at the origin. Often there is a second false peak at about twice the distance, a trace of which is indeed seen in fig. 2.

We now have to try and explain the genuine peaks by assuming a small number of fundamental spacings. There is no difficulty in this, in the present case, and the interpretations are indicated in fig. 2 (where AAB, for instance, means a peak resulting from spacing A twice plus spacing B once, in any order). The values of p_A and p_B are derived at once from the relative heights of peaks A and B: they can be converted to proportions, assuming of course that no other material unaccounted-for by these peaks is present in the sample. From the "higher-order" peaks we can derive the p_{rs}. For instance (where h represents peak height)

$$h_{AB} = K (p_A p_{AB} + p_B p_{BA}),$$

where K is a known proportionality factor.

Table 1
Spacings and intensities of diffraction maxima for 10 : 17.7 Å random mixture in proportion 3 :7 [from Brown and MacEwan, (6)]

Peak no.	d' (Å. U.)	I (pk. ht.)	$I/\lvert F_l \rvert^2$
1	17.7	215	80
2	9.195	10	72
3	5.567	15.4	23
4	4.425	2.9	17
5	3.490	10.6	14

Table 2
Measured and calculated heights of peaks on Fourier transform from Brown and MacEwan's data for diffraction by 70/30 (mica)-(glycerol-montmorillonite) interstratification

Peak	Calc. rel. ht.	Obs. rel. ht.
A	0.32	0.25
B	0.68	0.75
AA	0.10	0.16 (est.)
AB	0.43	0.33
BB	0.46	< 0.60
AAA	0.03	0
AAB	0.21	0.18 (est.)
ABB	0.45	0.29
BBB	0.01	0

Relative heights are measured from lower (smoothed) curve in fig. 2, using the proportions 68/32, as directly determined from the Fourier transforms.

We can obtain a series of equations of this nature, and have to find the best values of the p_{rs} to satisfy them, which we can do by trial and error (there is probably little point in using sophisticated mathematical techniques for this purpose, since very accurate agreement cannot be achieved). We naturally assume a completely random mixture to start with (for which $p_{AB} + p_{BB} = p_B$, $p_{BA} = p_{AA} = p_A$). In the present case, this at once gives an adequate agreement with measured values as shown in table 2.

We conclude that the scattering curve corresponds to a random mixture of 10.3 and 17.5 Å spacings in proportion 32 : 68[3]), a conclusion which is of course essentially correct.

G. Brown and R. Greene-Kelly (7) have given actual diffraction data from "partially collapsed" montmorillonite, which they show to be in good accord with predictions of the Hendricks-Teller theory. Their data may also be interpreted by the present direct method. Fig. 3 shows the Fourier transform

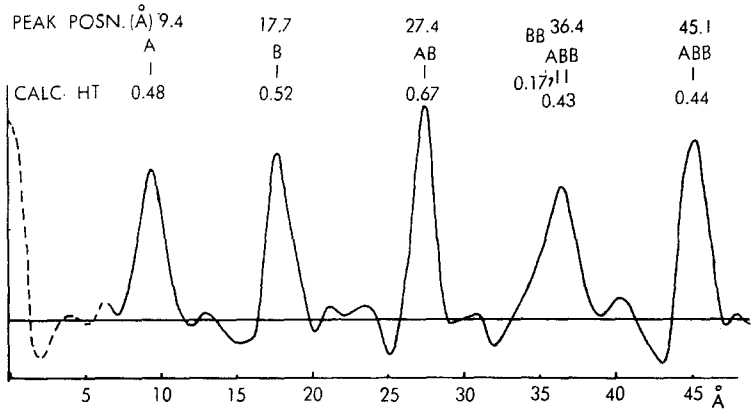

Fig. 3. Transform from observed intensities for a "partially collapsed" glycerol-montmorillonite.

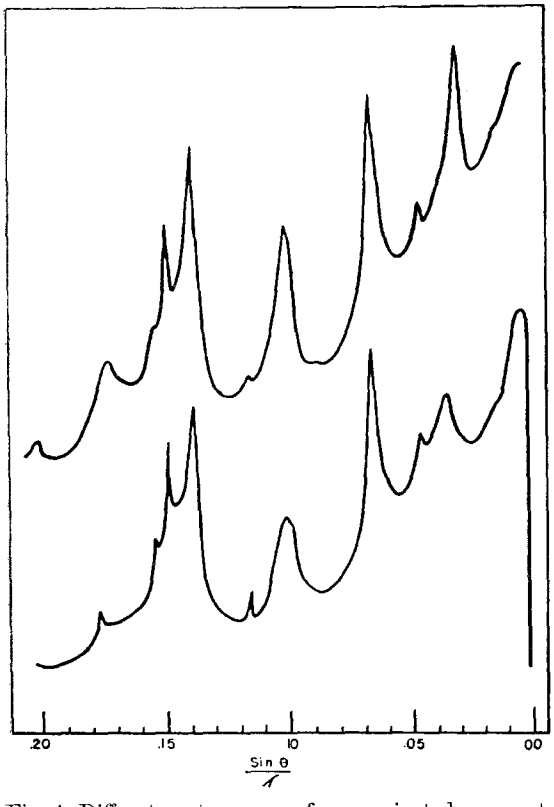

Fig. 4. Diffractometer curves for an oriented aggregate of clay. Above, before; below, after rapid heating to 450°. From Bradley (25).

for the case $p = 0.48$ (p = proportion of higher spacing = our p_B).

Measurement of the first-order peaks gives $p_B = 0.52$. Better agreement is found with the heights of the "combination peaks" if it is assumed that the sequence is not completely random, but that there is a tendency to an alternating structure $ABAB\cdots$. The heights written above the peaks are calculated with $p_{AB} = p_{BA} = 0.67$; $p_{AA} = p_{BB} = 0.33$ (for complete randomness, $p_{AB} = p_{BB} = p_B$; $p_{BA} = p_{AA} = p_A$). This tendency to alternation may well be a genuine effect; but in general Brown and Greene-Kelly's interpretation is well confirmed.

We now consider a much more complicated practical case, due to Bradley (25). Fig. 4, taken from Bradley's paper, shows X-ray diffractometer records of a well-oriented aggregate of a clay before (above) and after (below) rapid heating to 450° C. Fig. 5 shows the Fourier transforms derived from these curves.

The analysis of these transforms is complex and interesting, and may be carried out in considerable detail. The first step is to find out the correct zero line, which was done by the method already described. It is then possible to bring the two curves to a comparable scale by adjusting the zero peak to have the same height: the peak heights on the two curves may then be compared directly (this process assumes that in the two cases, the basal series of reflections represents the same quantity of diffracting material, i. e. that there has been no conversion of material into the amorphous, or non-lamellar form).

The peak at about 3.5 Å on both transforms is a "diffraction" peak, and is neglected. The other peaks on the "before heating" curve may then readily be interpreted as kaolin (A), mica (B), vermiculite and/or chlorite plus "second order" kaolinite ($C + AA$), montmorillonoid (D) (the material was treated with ethylene

[3]) A mean value from measurements of several peaks. From the A and B peaks alone, we obtain: 40 : 60 from the unsmoothed curve, 24 : 76 from the smoothed curve.

glycol, which gives a montmorillonoid spacing around 17 Å).

On rapid heating we expect the montmorillonoid spacing to pass to around 10 Å: a vermiculite spacing would shift to the same value. In fact, as shown in table 3, which gives a résumé of the measurements of these transforms, the *C* peak hardly changes; the *D* peak disappears and the *B* peak increases by approximately the height of the *D* peak. Clearly therefore the *C* peak is due to chlorite, not vermiculite, and the *D* peak to montmorillonoid. This interpretation is both qualitatively and quantitatively in accord with Bradley's conclusions.

The values of the p_{rs} shown in table 3 have been selected so as to give the best general agreement with peak heights. They show that the kaolin and mica are separate phases ($p_{AA} = 1$, $p_{BB} = 1$), but the chlorite and montmorillonoid are interstratified, not, however,

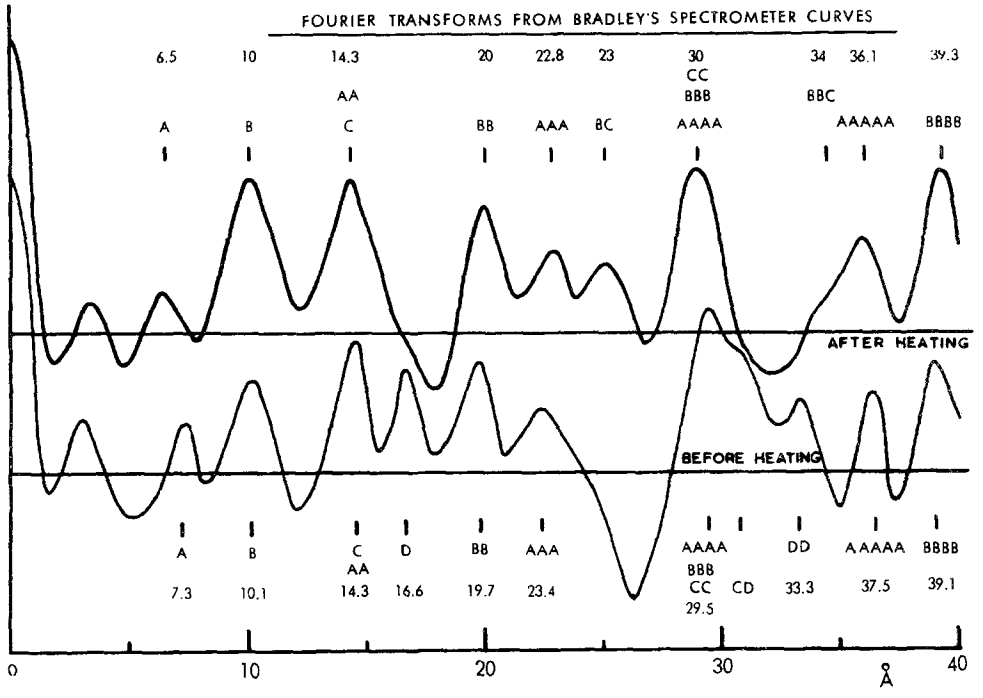

Fig. 5. Fourier transforms from curves of fig. 4 (note that the order is reversed). The numbers attached to the curves give peak-height readings in Å.

Table 3

Analysis of Bradley's spectrometer curves (Anal. Chem. **25**, 729 (1953), fig. 9, left hand curves).

(1) Mineral before heating			(2) Mineral after heating		
Peak	Obs. ht.	Calc. ht.	Peak	Obs. ht.	Calc. ht.
A (7)	0.16	(0.16)	*A* (7)	0.14	(0.14)
B (10)	0.28	(0.28)	*B* (10)	0.50	(0 50)
C + *AA* (14)	(*C*) 0.24	(0.24)	*C* + *AA* (14)	(*C*) 0.36	(0.36)
D (17)	0.32	(0.32)	*BB*	0.42	0.42
BB	0.34	0.28	*AAA*	0.26	0.14
AAA	0.20	0.16	*BC*	0.24	0.15
BBB + *CC* + *AAAA*	0.49	0.49	*BBB* + *CC* + *AAAA*	0.55	0.65
CD	0.37	0.16	*BBC*	0.11	0.16
DD	0.23	0.38	*AAAAA*	0.31	0.14
AAAAA	0.25	0.16	*BBBB* + *BCC*	0 53	0.46
BBBB	0.32	0.28			

$p_A = 0.16$ $p_B = 0.28$ $p_C = 0.24$ $p_D = 0.32$

$p_{AA} = 1$ $p_{BB} = 1$ $p_{CC} = 0.65$ $p_{DD} = 0.75$ $p_{CD} = 0.35$ $p_{DC} = 0.25$

$p_A' = 0.14$ [0.16] $p_B' = 0.50$ [0,60] $p_C' = 0.36$ [0.24]

$p_{AA}' = 1$ $p_{BB}' = 0.84$ [0.87] $p_{CC}' = 0.76$ [0.65] $p_{BC}' = 0.16$ [0.13] $p_{CB}' = 0.24$ [0.35]

Figures in square brackets are calculated from the data in section (1). See text.

completely randomly[4]). There is a marked tendency to segregation of the individual types of layers ($p_{CC} > p_C$ and $p_{DD} > p_D$).

It should be noted that, on heating, the montmorillonite-chlorite interstratification becomes effectively a mica-chlorite interstratification. Assuming that this happens, it is possible to calculate the expected values of p'_{BC} and p'_{CB}, where the primes indicate the "after-heating" values. They are close to the values determined directly from the Fourier transform of the material after heating. This comparison is shown in table 3, the values in square brackets being the calculated ones. This agreement provides very satisfactory confirmation of our suppositions regarding the nature of the changes occurring as a result of the heat treatment.

The conclusions drawn from the above treatment are, of course, in close agreement with Bradley's, which were reached without the aid of Fourier transforms; but the Fourier transform method leads directly to the result, and gives a certain amount of extra detail.

The values of p_A, p_B, etc. may be considered to represent actual proportions of different types of layers. It would be unwise, however, to attribute to them any absolute importance. They would represent true proportions if the different types of layer had identical structure factors (the structure factor for a mica type layer has been used throughout, in calculating the transforms). This is far from being the case. However, the quantities retain a relative value so long as the structure factors for each type of layer remain the same, i. e. an increase in p_r does really represent a corresponding increase in the true proportion of the r type of layer. Where this condition is not fulfilled, discrepancies must be expected. The fact, for instance, that p'_B is less than $p_B + p_D$ is probably due to a change in the structure factor of the B (chlorite) type of layer, occurring as a result of the heat treatment.

Fig. 6 (top curve) is a Fourier transform derived from a glycerol treated montmorillonite which has been partly dried. (The X-ray photographs were made by G. Brown.) We notice immediately the prominent peak C at 17.7 Å, corresponding to glycerol-montmorillonite. There are also two rather ill-developed peaks near 10 and 13 Å. It would clearly be an advantage here to get rid of the strong C and CC peaks and their associated diffraction. We therefore apply the procedure described in the last paragraph of section 5. The resulting curve is the lower one of fig. 6. It enables us to deduce the accurate spacings of peaks A and B (9.5 and 12.3 Å) and shows up clearly the "combination" peaks BB, AC, BC. This curve must be interpreted with caution, since it includes two peaks (at 7 and 21 Å), which have no ready interpretation and are almost certainly false. Moreover the curve descends steeply below zero for spacings greater than 30 Å, a clear indication that it is not fully accurate.

From the two curves we can readily deduce that:

(1) Glycerol-montmorillonite (C) is the chief spacing, amounting to about 70%. It is partially mixed, both because combination peaks occur, and because the CC peak is lower than C (the peak heigths are in the ratio p_{CC}, as has been demonstrated).

(2) The A spacing ("collapsed montmorillonite") occurs in admixture with C, and not to any appreciable extent alone (absence of peak AA).

(3) The B spacing occurs partially segregated, and partially in admixture with C (presence of BB and BC).

It should be noted that the removal of peaks C, CC, etc. does not remove the peaks of type AC, BC, etc.

The few examples discussed above have been chosen to illustrate the practical application of this method. The author has experimented widely with it, and is convinced that it can be a valuable aid in the interpretation of all manner of interstratification phenomena. The method has many of the advantages of that of Patterson in structure analysis: that it is direct, and that it shows at a glance the totality of the information available from the diffraction data. In comparison with a Patterson diagram, however, the interpretation of a one-dimensional Fourier transform usually involves fewer hypotheses.

The chief disadvantage is that, in theory, the layers must all have the same structure factor. It has been shown, however, in the present paper, that in practice useful information can be derived even if there are great differences in structure factor.

Bradley has shown, in several publications (26, 27) that one may go a long way in the interpretation of the X ray diagrams by a more or less intuitive appreciation, based on a familiarity with the nature of the diffraction

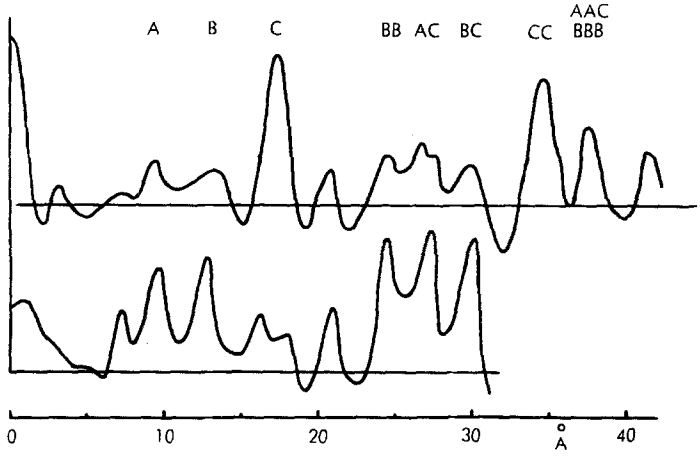

Fig. 6. Above, Fourier transform from glycerol-treated montmorillonite, partly dried. Below, the same, after removal of peaks at 17.7 Å, and multiples (C, CC).

[4]) The term "completely randomly" merely indicates the absence of any tendency either to segregation (*like* layers succeeding each other), or to alternation (*unlike* layers succeeding each other).

process. The author has applied the Fourier transform method to many of the cases analysed by Bradley, and has always found it to give results in substantial agreement with his. There are differences in detail, for instance in the exact proportions of the components; and the Fourier method often gives extra information which appears plausible. Both the Fourier method and the "intuitive" method can work well, but the first mentioned is decidedly more direct and immediate in its application.

7. Methods of calculation

The calculation of a transform of this nature is conveniently done as follows. We construct first a preliminary table (table 4). Columns 1 and 2 are the measured quantities-intensities and spacings of lines [these particular values are for a Kinnekulle clay, from A. M. Byström (28)]. In column 3, the estimated intensities have been converted to a numerical scale (they may of course be so measured in the first place).

Column 4 gives the angular intensity factor (Lorentz, polarisation and geometrical), column 5 the layer structure factor, and column 6 the intensities corrected by means of these factors. They are further multiplied by a suitable arbitrary number to give convenient values for manipulation. Column 7 is the square root of column 6, again with a suitable factor, and rounded off to give convenient whole numbers. These numbers are the amplitudes of the Fourier terms; we will call them A_1, A_2, etc. Finally, column 8 gives $360/d'$, i. e. it is a reciprocal spacing. We will call it d'^*. If d' and R are in Ångströms, then the Fourier transform is simply $\Sigma_r A_r \cos(d_r'^* R)$, where $(d_r'^* R)$ is expressed in degrees.

For making these calculations, it is invaluable to have a table giving cosines to two figures at degree lines in table 4. Thus we simply have to multiply the values of column 8 successively by 1, 2, 3 . . . (corresponding to values of R in Å: we could of course take larger or smaller intervals as desired, but usually it is convenient to calculate at 1 Å intervals), find the cosines of these quantities, multiply each by its A_r, and sum for each value of R. Table 5 shows some of this work. Corresponding to each value of r we have two columns, one for $(d_r'^* R)$, and one for $A_r \cos(d_r'^* R)$ (which can be calculated from $d_r'^* R$ in one operation, using a slide rule). The latter quantity is rounded off to the nearest whole number. The final column gives the sum of these quantities, and is the ordinate of the transform for the corresponding value of R.

Table 4

Preliminary calculations for Fourier transform. Kinnekulle clay, type 1 (spacings and intensities from Byström (28)

	(1) $I_{est.}$	(2) d'	(3) I (num.)	(4) Ξ	(5) $\lvert F_l \rvert^2$	(6) $\frac{1000\, I}{\Xi \lvert F_l \rvert^2}$	(7) $\frac{2\times}{\sqrt{(6)}}$ (Ar)	(8) $\frac{360}{d'} = d'^*$
1st term	*vs*	18.0	32	22.5	4800	0.29	1(4)*	20.00
2nd term	*s*	9.0	16	11.6	12	117	20	40.00
3rd term	*w*	5.71	1	7.1	530	0.26	1	63 05
4th term	*s*	4.44	16	5.5	70	41	13	81.08
5th term	*vs*	3.42	32	4.2	360	21	9	105.26
6th term	*s*	2.93	16	3.4	600	8	6	122.87
7th term	*w*	2.55	1	2.9	220	1.5	2	141.18
8th term	*s*	1.92	16	2.2	600	12	7	187.5

* The value 4 was used instead of 1, as it was considered that the intensity was probably underestimated for this term.

Note that the values of $\lvert F_l \rvert^2$ used here do not correspond exactly with any of the graphs of fig. 8.

There are as many terms in the summation as there are intervals, and for angles up to several thousand degrees. This can easily be prepared before-hand.

Figure 7 shows a simple device which speeds up the process by eliminating the calculation of $d_r'^* R$. The angle $d_r'^*$ is set off first by means of the marker M, the multiples of this angle are obtained successively by rotating the disc D so as to bring the point B to A. The value of $A_r \cos(d_r'^* R)$ is then read off directly at the point where the circle C cuts the scale S (the circle C' is in a contrasting color and gives negative values). There is a separate scale for each value of A_r. I have found that twenty such scales, to cover values from 1 to 20, give adequate accuracy.

With this device the intermediate columns are eliminated. A calculation of the type shown, up to $R = 40$, can easily be done using it in an hour or so.

Table 5

Part of final table for calculation of Fourier transform from data in columns (7) and (8) of table 4

R	1st term α	1st term Y	2nd term α	2nd term Y	3rd term α	3rd term Y	4th term α	4th term Y	5th term α	5th term Y	6th term α	6th term Y	7th term α	7th term Y	8th term α	8th term Y	Σ
0		4		20		1		13		9		6		2		7	62
1	20	4	40	16	63	0	81	2	105	$\bar{2}$	123	$\bar{3}$	141	$\bar{2}$	188	$\bar{7}$	8
2	40	3	80	3	126	$\bar{1}$	162	$\bar{12}$	210	$\bar{8}$	246	$\bar{3}$	282	0	375	7	11
3	60	2	120	$\bar{10}$	189	$\bar{1}$	243	$\bar{6}$	316	$\bar{6}$	369	6	424	1	563	$\bar{6}$	20
4	80	1	160	$\bar{19}$	255	0	324	10	421	5	491	$\bar{4}$	565	$\bar{2}$	750	6	3

$\alpha = (d_r'^* R)$ in degrees $\qquad Y = A_r \cos(d_r'^* R)$

$\Sigma = \Sigma_r A_r \cos(d_r'^* R)$

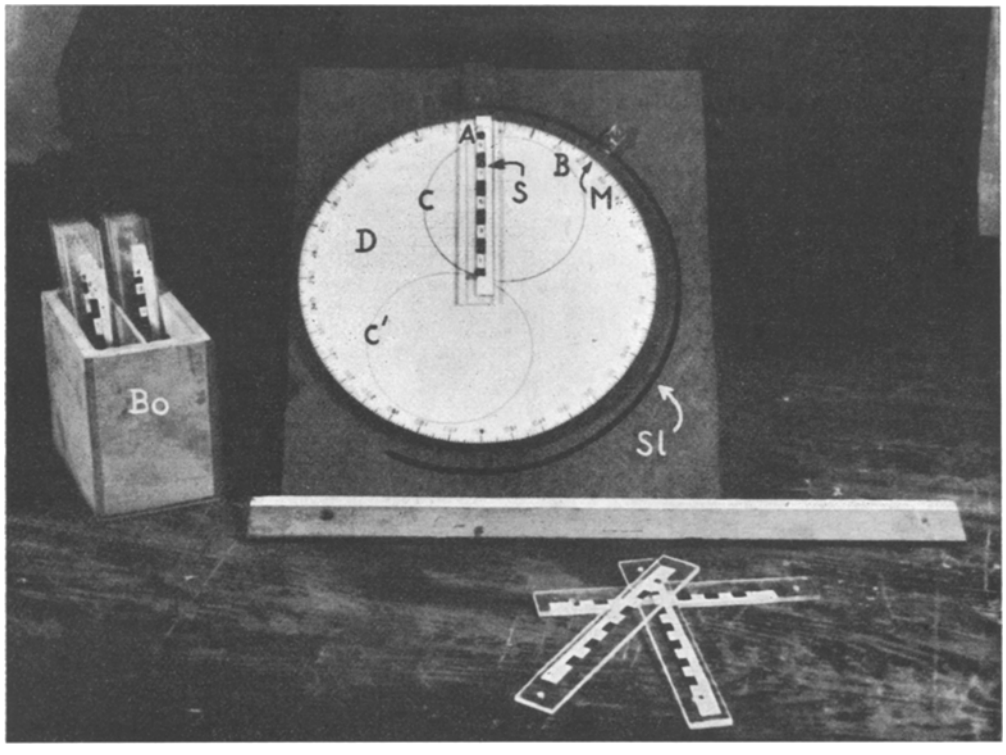

Fig. 7. Apparatus for calculating Fourier transforms. *M*-marker for setting off angle, rotating around slot *Sl*. *D*-disc, graduated in degrees, and rotated around axis *Ax*. *S*-transparent scale, graduated in units. 20 of these are available, reading from a maximum of 1, up to a maximum of 20. The graduations are: 0 to $^1/_2$ (reading 0); $^1/_2$ to $1^1/_2$ (reading 1); $1^1/_2$ to $2^1/_2$ (reading 2); and so on. *Bo*-box of scales. Three scales are seen lying in front of the apparatus.

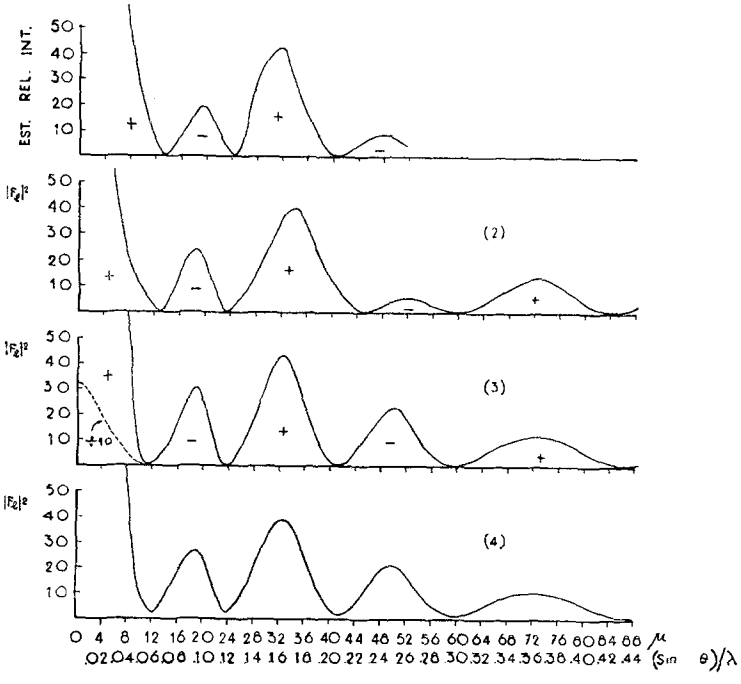

Fig. 8. Square of structure factor for basal reflexions from montmorillonite (and similar) layers.
(1) Experimental, from Bradley (29).
(2) Calculated, with allowance for interlamellar material. (See text.)
(3) Calculated as above, without allowance for interlamellar material.
(4) As (3), averaged continuously over 4 units of μ.

8. The layer structure factor

The calculation of this quantity necessarily involves certain assumptions. We must suppose that the type of layer is known, at least to a first approximation. The structure factor can then be calculated as a continuous function of Θ, or of $\mu = 100/d'$. If, for instance, the structure is centrosymmetrical (in the linear projection), and if it has N_r atoms with coordinate z_r and atomic scattering factor $f_r(\mu)$, then the layer structure factor is given by

$$F_l(\mu) = \Sigma_r N_r f_r \cos 2\pi (\mu z/100).$$

The more general form of the formula can easily be worked out. The quantity we are interested in is $|F_l|^2$, and this can be represented by means of a graph.

For the mineral montmorillonite, Bradley (29) has already given a useful graph of this quantity, based on experimentally measured intensities for montmorillonite-organic complexes. This curve is reproduced in fig. 8 curve (1). This figure also shows for comparison three calculated curves for montmorillonite. The curves are very similar, and they will do, to a sufficient order of approximation, for all other layers of the same general type, micas, pyrophyllite, talc, etc. For chlorites, they are less accurate, and for kaolin type minerals quite inaccurate. Use of the wrong curve (as we have seen) will not affect the determined interlayer distances very much, but will affect the estimated quantities.

Curve (2) is calculated for layers with interlamellar material, of the type of water molecules, organic molecules, etc. This has been done (the correction is only a rough one) by superposing the average electron density of a close-packed layer of water molecules on the entire layer, and using, instead of the true electron content of the atoms, the "electron contrast", i. e. the true electron content minus the content of "background electrons" in the volume of the atoms.

Curve (3) is calculated using the true electron contents of the atoms. Curve (4) is curve (3), averaged continuously over 4 units of μ, so that it never reaches zero. One sometimes finds lines of appreciable intensity where there ought to be a zero of F_l. This may, of course, indicate that F_l is wrongly calculated. However, it seems probable that, because of the angular spread of the X-ray beam, and the width of the reflections, there are no zeros of the effective curve of F_l^2. The procedure of averaging over a small region may therefore give rather more realistic values of this quantity.

Summary

The study of interstratified clay minerals and similar systems by X-rays requires some means of rapidly estimating the interlayer spacings present, their proportions and the manner of their sequence. For this purpose, a simplified one-dimensional Fourier transform is here suggested. For its calculation, only the positions ("effective spacings") and intensities of the basal diffraction peaks need to be known, and these can readily be obtained from orientation powder diagrams or spectrometer recordings. The method of calculation is here fully described, and illustrated by practical examples.

Zusammenfassung

Zum Studium von Tonmineralien und ähnlichen Substanzen mit Schichtstruktur mittels Röntgenstrahlen ist es notwendig, eine Methode anzuwenden, die uns die vorkommenden Zwischenschichtabstände, deren Häufigkeit und Folge einfach und bequem zu schätzen erlaubt. Zu diesem Zweck wird hier eine vereinfachte Form der eindimensionalen Fouriertransformierten vorgeschlagen. Zur Berechnung dieser Funktion braucht man nur die Lagen („effektiven Abstände") und Intensitäten der Basis-Interferenzen zu kennen, und diese sind leicht aus orientierten Pulver-Diagrammen oder den Spektrometerregistrierungen zu erhalten. Die Methodik der Rechnungen wird ausführlich beschrieben und mit Beispielen aus der Praxis erläutert.

References

1) Brindley, G. W. (Editor), X-ray identification and structure of clay minerals (London 1951).
2) Garcia Vicente J., Estructura cristalina de la areilla (Madrid 1951).
3) Jasmund, K., Die silikatischen Tonminerale (Weinheim 1951).
3a) MacEwan, D. M. C., J. Soil Sci. **1**, 90 (1949).
4) Salt, F. E., Clay Mins. Bull. **1**, 55 (1947) (discussion).
5) Hendricks, S. B. and E. Teller, J. Chem. Phys. **10**, 47 (1942).
6) Brown, G. and D. M. C. MacEwan, J. Soil Sci. **1**, 239 (1950). (See also chapter by Brown and MacEwan in Ref. 1.)
7) Brown, G. and R. Greene-Kelly, Acta Cryst. **7**, 101 (1954).
8) MacEwan, D. M. C., Nature **171**, 616 (1953).
9) MacEwan, D. M. C., Bull. 169, Calif. Dept. of Nat. Resources, p. 127 (1955).
10) Brindley, G. W. and J. Goodyear, Min. Mag. **28**, 407 (1948).
11) Ref. 1, p. 86.
12) Stephen, I. and D. M. C. MacEwan, Clay Mins. Bull. **1**, 157 (1951).
13) MacEwan, D. M. C., Trans. Faraday Soc. **44**, 349 (1948).
14) Greene-Kelly, R., Trans. Faraday Soc. **51**, 412 (1955).
15) Hofmann, U., Ergeb. exakt. Naturw. **18**, 229 (Berlin 1939).
16) Riley, H. L., Fuel. **24**, 8 and 43 (1945).
17) MacEwan, D. M. C. and O. Talibuddin, Bull. Soc. Chim. France **16**, D 37 (1949).
18) Nagelschmidt, G., J. Sci. Instr. **18**, 100 (1941).
19) Mitchell, W., Clay Mins. Bull. **2**, 76 (1954).
20) Brown, G., J. Soil Sci. **4**, 229 (1953).
21) MacEwan, D. M. C., J. Soc. Chem. Ind. **65**, 298 (1946).
22) Brindley, G. W. and J. Méring, Acta Cryst. **4**, 441 (1951).
23) Méring, J., Acta Cryst. **2**, 371 (1949).
24) James, R. W., Optical principles of the diffraction of X-rays (London 1948).
25) Bradley, W. F., Anal. Chem. **25**, 727 (1953).
26) Bradley, W. F., Trans. 4th Int. Congr. Soil Sci., Amsterdam **1**, 101 and 425 (1950).
27) Bradley, W. F., Sedim. Petr. **24**, 242 (1954).
28) Bystrom, A.-M., Nature **173**, 783: and Geol. Fören. i Stockh. Förh. **76**, 87 (1954).
29) Bradley, W. F., Am. Min. **30**, 704 (1945).